

A Reactive Molecular Dynamics Study of Phenol and Phenolic Polymers in Extreme Environments

Keith Jones^{1,a)}, J. Matthew D. Lane¹ and Nathan W. Moore¹

¹*Sandia National Laboratories, Albuquerque, NM 87185 USA*

^{a)}Corresponding author: keijone@sandia.gov

Abstract. Phenolic polymers are key components in carbon composites used in heat shielding due to their ablative properties, and are oftentimes exposed to extreme conditions such as heating and shock. Our ability to model these systems requires an understanding of shock induced chemical pathways. In this work, the ability of three parametrizations of the ReaxFF classical MD potential were compared in their ability to model phenolic polymers under shock induced chemistry. We calculated the activation energies associated with both the formation of water, and the liberation of volatile compounds via an Arrhenius analysis of several constant temperature pyrolysis simulations. The activation energies for all three parametrizations are in agreement with the experimental thermogravimetric analysis (TGA) results. We also studied phenol, a relevant model system with a well-defined structure. We observed that the density of phenol in one parametrization, for six temperatures ranging from 123 K to 423 K, was in closer agreement with the experimental results. The accuracy of the density of phenol at various temperatures serves as an indicator for the ability of a given parametrization to predict density of a phenolic polymer under shock.

INTRODUCTION

Reactive molecular dynamics (MD) can provide insight into the processes that occur during heating and shock, as well as the relationship between the molecular structure and the density, shock response, and mechanisms of pyrolytic breakdown—a valuable link between microscopic properties and macroscopic observables. For example, depending on the curing conditions, phenolic polymers can vary greatly in crosslink extent, initial density, stoichiometry, and molecular structure [1, 2]. Each of these factors modulates the hydrogen bonding topology, which has been shown with MD to play a role in the thermal-mechanical properties of phenolic polymers [3]. Hydrogen bonding interactions are strong intermolecular interactions that phenolic polymers exhibit due to the hydroxyl groups present throughout the structure.

A reactive force field that can also model mechanical compression is necessary to elucidate the chemical pathways associated with the "phase change" observed by Carter and Marsh [4] in many polymers between 20 and 30 GPa. In this work, we investigate the ability of three ReaxFF MD parametrizations to model compression and to model chemistry during pyrolysis that can occur during high pressure shock in phenolics. ReaxFF is a bond order MD potential that handles chemistry [5], with parametrizations for various combinations of elements and conditions. Phenolic polymers have been studied with molecular dynamics in the past, under both reactive [6, 7, 8, 9, 10] and non-reactive [3, 11, 12, 13] conditions. A previous MD study, which modeled phenolic polymers under shock using a non-reactive potential [3], concluded that the experimentally observed phase transition in the Hugoniot, characterized by a large volume change, was not reproducible with the non-reactive force field because this change is due to a chemical transformation.

We chose the ReaxFF parametrizations by Chenoweth et al. [14], Mattsson et al. [15], and a hybrid parametrization that we developed specifically for this work which capitalizes on the properties of the Chenoweth and Mattsson parametrizations. The Chenoweth parametrization is commonly used to study hydrocarbon reactivity and oxidation and has been employed in the past to study phenolic pyrolysis [6, 7, 8, 9, 10, 16]. The Mattsson parametrization has been utilized in the past for simulating polymers containing only hydrogen and carbon (i.e. non-hydrogen bonded systems) subject to high-rate thermal degradation [17] and under shock induced chemistry, up to 60 GPa, in agreement with experimental results [15]. Our hybrid ReaxFF parametrization refines the accuracy of the intermolecular inter-

actions of the Mattsson parametrization by removing the O-H — O hydrogen bonding parameters from the Mattsson parametrization and replacing them with those of the Chenoweth parametrization.

Using the three ReaxFF parametrizations, we calculated the activation energies associated with the formation of water as well as the liberation of volatile compounds and compared the results with available experimental studies. Water is a common byproduct from both pyrolysis as well as the curing process of phenolic polymers, and the formation kinetics of water during phenolic pyrolysis have been studied in the past [6, 7]. Experimental activation energies are typically extracted via the manipulation of the mass loss curve acquired from thermogravimetry. The rationale for the second process lies in the fact that the experimental mass loss occurs due to the liberation of volatile compounds.

In addition to the chemical reactivity studies, MD simulations were carried out in the non-reactive regime to probe the ability of each ReaxFF parametrization to model the intermolecular interactions inherent in phenolic polymers. We studied phenol, an appropriate model system that exhibits many of the same intermolecular interactions that exist in phenolic polymers due to the fact that phenol is the building block of phenolic polymers. Experimentally, phenolic polymers are known to have many points of both structural and stoichiometric uncertainty. This is due to the large number of synthesis conditions that affect the final state of the polymer [1, 2, 18, 19], and that the major commercial suppliers of liquid resins do not publish trade secrets.

Crystalline phenol was chosen to test the ability of each parametrization to accurately model hydrogen bonding interactions. Crystalline phenol arranges itself into a 3-fold, H-bonded helix (Fig 1) along the crystallographic b-axis [23]. The stability of this structure at the experimental temperature serves as an indicator of the level of accuracy of the hydrogen bonding interactions of a given potential.

Phenol was also studied at higher temperatures in order to determine which parametrization could most accurately model phenolics under compression at high temperatures.

METHODOLOGY

We carried out phenolic pyrolysis with all three ReaxFF parametrizations using constant temperature, constant volume MD at temperatures between 2000 K and 3250 K using the LAMMPS [20] MD package. An amorphous, 1776 atom system of 16 linear chains, each containing 8 monomeric subunits, representing a phenolic polymer was used. We equilibrated 15 unique instances of this small system, repeated the procedure with each, averaging over them to improve the statistics. Periodic boundary conditions, a Berendsen thermostat, and a 0.25 fs timestep were employed. The simulations ran from tens to hundreds of picoseconds, depending on the temperature.

The kinetics of two processes were studied: the formation of water, and the liberation of volatile compounds. Volatile compounds were defined by a mass cutoff based on the heaviest compounds observed experimentally [21, 22], a number slightly greater than the mass of cresol (methylphenol). It was also verified that using the mass of either phenol (lighter) or xylenol (heavier) as the mass cutoff did not significantly affect the value of the activation energies. The activation energies associated with the liberation of volatile compounds will also be referred to as "global activation energies".

Crystalline phenol was equilibrated with each ReaxFF parametrization for 125-350 ps at 123 K and ambient pressure, beginning with the experimental x-ray crystal coordinates from [24], and the resulting density evaluated. The degree of crystallinity was determined by evaluating the mean squared displacement and diffusion coefficient of the system, as well as by qualitative observation of the time evolution of the 3-fold, hydrogen-bonded helix. The experimentally determined unit cell contains six molecules. This was replicated 5-fold in each direction, for a final system of 9750 atoms. Periodic boundary conditions, a Nose-Hoover thermostat/barostat, and a 0.1 fs timestep were employed.

For the higher temperature simulations, phenol was equilibrated at 5 different temperatures between 300 and 425 K for which experimental data are available using the same equilibration procedure that was used for the crystalline phenol. In addition to the experimental data, a NIST model was used for comparison. Specifically, the NIST ThermoData Engine [26, 27] was accessed via the NIST Web Thermo Tables application [28], which extrapolates and interpolates a wide range of available experimental data, using the EOS code REFPROP [29]. The density-temperature curve along the liquid vapor coexistence was extracted from the NIST model data, and compared with the MD results up to the critical temperature (694 K). Pressures ranged from ambient to 55 atm along the liquid/vapor coexistence.

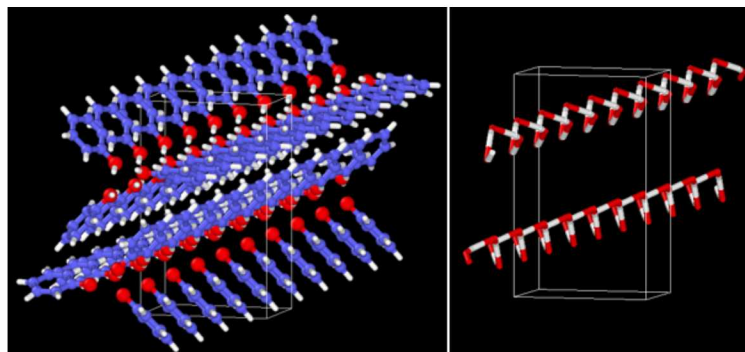


FIGURE 1. OVITO [25] visualization of the experimental x-ray crystal structure of phenol from [24]. The unit cell is replicated along the crystallographic b-axis to highlight the 3-folded helix. The image on the left contains all of the atoms. The image on the right only contains the hydrogen bonding atoms. The level of diffusion of this system during the equilibration is a metric for the ability of a ReaxFF parametrization to accurately model hydrogen bonding interactions relevant for shock.

RESULTS

Formation rates of water and of volatile compounds were extracted as a function of time for each simulation, enabling the extraction of rate constants and activation energies. These energies were averaged over 15 unique instances of the amorphous 16-chain system with a density of 1.25 g/cc (a typical density of a phenolic polymer), and compared with experimental results.

The order of both processes in the concentration of the reactant was not determined, because this dependence is irrelevant, as we carried out all analyses in the limit of constant reactant concentration, where the rate of product formation is approximately constant as can be seen in the left panel of Fig. 2. The rate equation below is expressed as a first order decomposition:

$$\frac{d[\text{H}_2\text{O}]}{dt} = A[\text{Phenolic}] \cdot \exp\left(-\frac{E_a}{RT}\right) \quad (1)$$

$$\ln k = \ln B - \frac{E_a}{RT} \quad (2)$$

Eq. 1 can be represented as Eq. 2, where $[\text{H}_2\text{O}]$ is the concentration of water and k is an effective rate constant, equal to the rate during the initial stage of pyrolysis where the concentration of phenolic, $[\text{Phenolic}]$ is approximately constant. The initial rates of the two processes of interest, i.e. water formation and the appearance of volatile compounds, were determined for each constant temperature pyrolysis simulation and used to build the Arrhenius plot (right panel, Fig 2) from which activation energies could be extracted. We chose the more standard natural logarithm of the rate constant for the Arrhenius plot, and recalculated the values cited from previous work [6, 7] in Table 1. Activation energies were evaluated for each of the 15 instances of the system. The average values are reported here with the error bars reported as the standard deviation. Other means of determining the activation energy were tested, all yielding the same results within uncertainties.

As can be seen in Table 1, the Chenoweth activation energies were consistently higher than with both the hybrid and the Mattsson parametrizations. However, all MD parametrizations yielded activation energies for water formation as well as global activation energies in agreement with experimental results, which vary widely. The wide range of the experimental data could be due to several factors. Experimentally, the activation energies of phenolic pyrolysis have been shown to vary with heating rate [30] as well as the temperature regime [31, 32] in which the analysis is carried out. Furthermore, the curing conditions for the phenolics in each study were likely not identical. Additional work is needed to compare reaction energies and activation barriers for specific, common product formation pathways using the various parametrizations with electronic structure calculations.

Phenol was studied in the non-reactive regime to determine which ReaxFF parametrization most accurately models intermolecular interactions in phenolic polymers. After equilibrating crystalline phenol using the Mattsson and Chenoweth parametrizations, it was observed that the Mattsson parametrization retains the experimental density

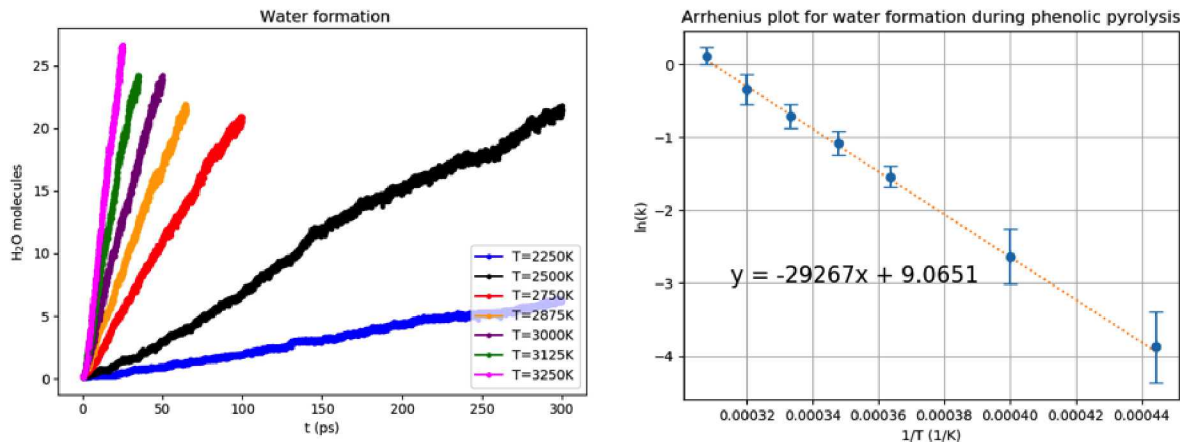


FIGURE 2. Arrhenius analysis data. The image on the left shows the water evolution curves from MD simulations used to extract rate constants. The image on the right shows an Arrhenius plot.

TABLE 1. Phenolic pyrolysis activation energies.

Reference	E_a (H ₂ O) (kJ/mol)	E_a (Global) (kJ/mol)
Exp [32]	—	223-305
Exp [31]	—	74-198
Exp [30]	—	192-293
MD [6]	332(64)	—
MD [7]	286(46)	—
Chenoweth (this work)	246(23)	301(32)
Hybrid (this work)	135(5)	210(12)
Mattsson (this work)	130(6)	191(13)

of 1.19 g/cc to within 0.01 g/cc, but does not retain the crystal structure. The system amorphized significantly, and exhibits liquid-like behavior as indicated by the diffusion coefficient of $4.1 \times 10^{-4} \text{Å}^2/\text{ps}$. The left panel of Fig. 3 illustrates how far the three-fold helix has deviated from the x-ray crystal structure.

The Chenoweth parametrization retains the crystallinity as shown in Fig 3, and exhibits solid-like behavior as demonstrated in the mean squared displacement. However, the system densified by more than 20 percent of the experimental value to 1.43 g/cc.

In order to retain the crystallinity and the density of the system simultaneously, the hydrogen bonding parameters from the Mattsson parametrization were removed and replaced with those of the Chenoweth parametrization. The new hybrid parametrization capitalizes on the ability of the Mattsson parametrization to maintain reasonable densities and on the ability of the Chenoweth parametrization to accurately represent hydrogen bonding interactions. Fig. 3 demonstrates that the hybrid parametrization maintains the crystal structure. This new parametrization also maintains the experimental density.

Fig. 4 demonstrates that our hybrid parametrization accurately reproduces the intermolecular interactions that are important for studying phenolic polymers under shock. The hybrid parametrization most accurately models phenol across a range of temperatures, in agreement with experimental data [33, 34, 35] as well as the NIST model of the liquid/vapor coexistence curve, which spans a greater temperature range, up to the critical temperature. Depending on the equilibration strategy, the hybrid parametrization can model phenol in either the liquid or vapor phase when the system is equilibrated to a temperature and pressure on the coexistence curve.

It should be noted that investigation of the water formation mechanisms with our new hybrid parametrization revealed the existence of an overly stable intermediate that lowered the energy barrier of this process. An additional ReaxFF parameter, p_{ovun3} , was replaced for that of the Chenoweth parametrization. This intermediate no longer forms, and the conclusions of this work remain unchanged. The water activation energy for the new hybrid rose to 170 kJ/mol,

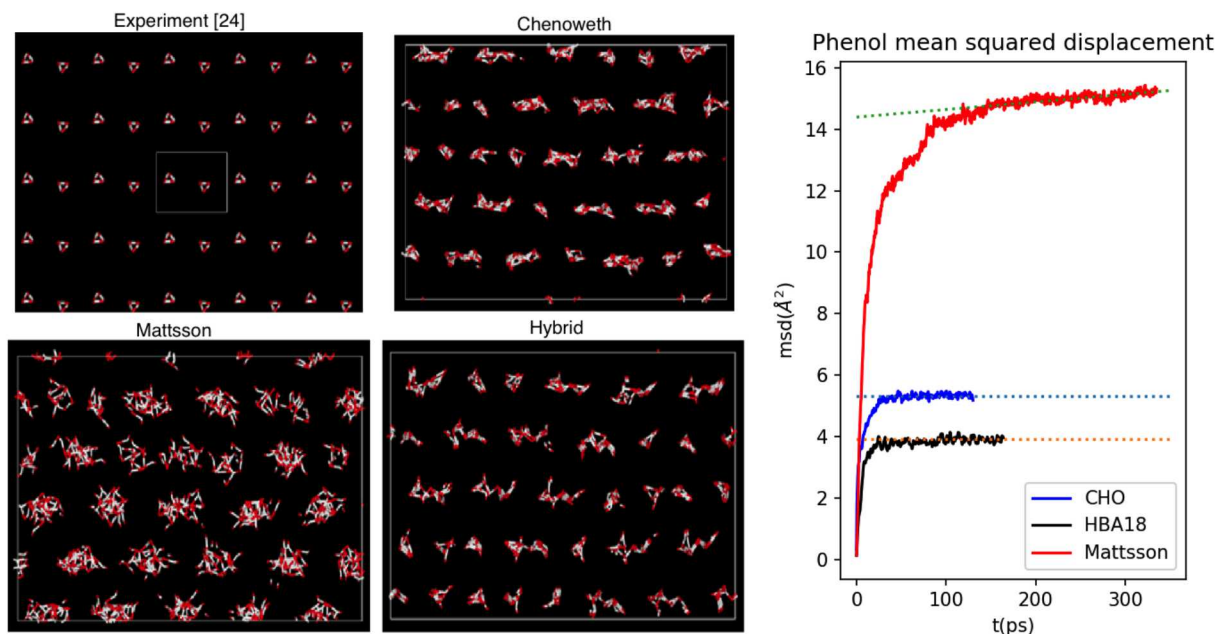


FIGURE 3. Left panel: visualization of the three fold hydrogen-bonded helix of crystalline phenol near the end of the equilibration with the three ReaxFF parametrizations. The viewpoint is oriented parallel to the crystallographic b-axis. The image in the upper left was produced using the experimental x-ray crystallography coordinates [24]. The Mattsson parametrization does not retain the crystallinity, unlike the Chenoweth and hybrid parametrizations. Right panel: mean squared displacement of atoms in phenol during equilibration at 123 K and ambient pressure. Phenol equilibrated with the CHO and hybrid parametrizations exhibit solid-like behavior, whereas the phenol equilibrated with the Mattsson parametrization exhibits liquid-like behavior, with a diffusion coefficient of $4.1 \times 10^{-4} \text{Å}^2/\text{ps}$ based on the slope of the fit line shown in the figure.

still lower than that of the Chenoweth, although closer, and still within the range of experimental values.

CONCLUSIONS

We used classical MD and the ReaxFF potential to model phenolic polymers. Three parametrizations were compared in their ability to model the chemical reactions that occur during pyrolysis and to model mechanical compression due to shock. All three ReaxFF parametrizations are comparable for pyrolysis and chemistry, based on a comparison with the available experimental activation energies determined by TGA. However, our new hybrid parametrization is the most ideal ReaxFF parametrization for studying shock, due to its ability to also accurately model hydrogen bonding interactions and reproduce densities of a model system relevant to phenolic polymers across a range of temperatures.

ACKNOWLEDGMENTS

Sandia National Laboratories is a multi-mission laboratory managed and operated by National Technology and Engineering Solutions of Sandia, LLC., a wholly owned subsidiary of Honeywell International, Inc., for the U.S. Department of Energy's National Nuclear Security Administration under contract DE-NA0003525.

REFERENCES

- [1] J. Bouajila, G. Raffin, H. Waton, C. Sanglar, J. O. Paise, and M. F. Grenier-Loustalot, *Polymers and Polymer Composites* **11**, p. 233 (2003).
- [2] N. Gabilondo, M. Larranaga, C. Pena, M. A. Corcuera, J. M. Echeverria, and I. Mondragon, *J. Appl. Polym. Sci.* **102**, 2623–2631 (2006).

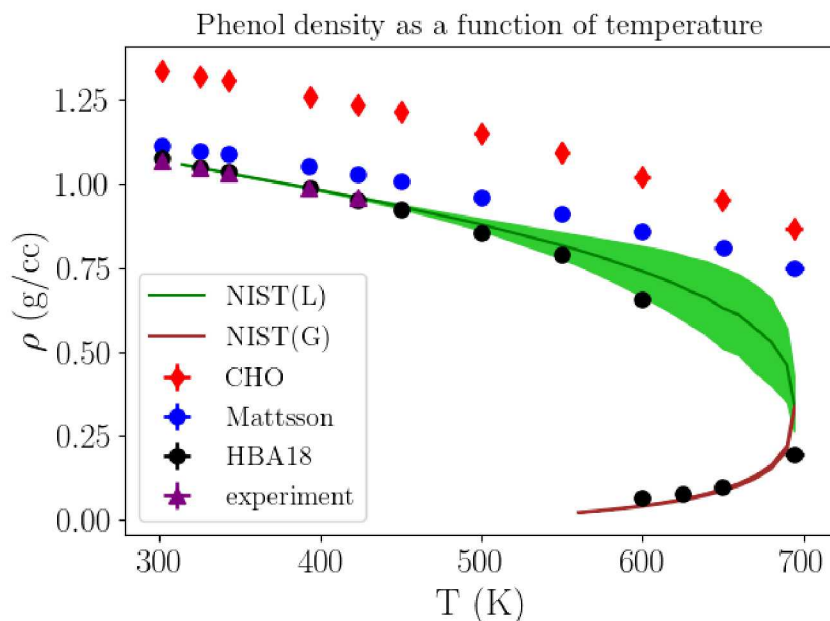


FIGURE 4. Phenol density as a function of temperature. The green and brown curves represent the NIST model for the liquid (green, uncertainty region shaded) and vapor (brown) coexistence. (Color available online).

- [3] J. D. Monk, E. W. Bucholz, T. Boghoozian, S. Deshpande, J. Schieber, C. W. Bauschlicher, Jr., and J. W. Lawson, *Macromolecules* **48**, 7670–7680 (2015).
- [4] W. J. Carter and S. P. Marsh, *Hugoniot equation of state of polymers* (University of California Press, Berkeley, 1995).
- [5] A. C. T. van Duin, S. Dasgupta, F. Lorant, and W. A. Goddard, III, *J. Phys. Chem. A* **105**, 9396–9409 (2001).
- [6] D. Jiang, A. C. T. van Duin, W. A. Goddard, III, and S. Dai, *J. Phys. Chem. A* **113**, 6891–6894 (2009).
- [7] T. G. Desai, J. W. Lawson, and P. Koblinski, *Polymer* **52**, 577–585 (2011).
- [8] Y. Zhong, X. Jing, S. Wang, and Q.-X. Jia, *Polym. Deg. and Stability* **125**, 97–104 (2016).
- [9] T. Qi, C. W. Bauschlicher, Jr., J. W. Lawson, T. G. Desai, and E. J. Reed, *J. Phys. Chem. A* **117**, 11115–11125 (2013).
- [10] A. Harpale, S. sawant, R. Kumar, D. Levin, and H. B. Chew, *Carbon* **130**, 315–324 (2018).
- [11] J. D. Monk, J. B. Haskins, C. W. Bauschlicher, Jr., and J. W. Lawson, *Polymer* **62**, 39–49 (2015).
- [12] A. R. Pawloski, J. A. Torres, P. F. Nealey, and J. J. de Pablo, *J. Vac. Sci. Technol. B* **17**, p. 3371 (1999).
- [13] Y. Shudo, A. Izumi, K. Hagita, T. Yamada, K. Shibata, and M. Shibayama, *Macromolecules* **51**, 6334–6343 (2018).
- [14] K. Chenoweth, A. C. T. van Duin, and W. A. Goddard, III, *J. Phys. Chem. A* **112**, 1040–1053 (2008).
- [15] T. R. Mattsson, J. M. D. Lane, K. R. Cochrane, M. P. Desjarlais, A. P. Thompson, F. Pierce, and G. S. Grest, *Phys. Rev. B* **81**, p. 054103 (2010).
- [16] C. W. Bauschlicher, Jr., T. Qi., E. J. Reed, A. Lenfant, J. W. Lawson, and T. G. Desai, *J. Phys. Chem. A* **117**, 11126–11135 (2013).
- [17] J. M. D. Lane and N. W. Moore, *J. Phys. Chem. A* **122**, 3962–3970 (2018).
- [18] R. A. Haupt and T. Sellers, Jr., *Ind. Eng. Chem. Res.* **33**, 693–697 (1994).
- [19] S. So and A. Rudin, *J. Appl. Polym. Sci.* **41**, 205–232 (1990).
- [20] S. J. Plimpton, *J. Comp. Phys.* **117**, 1–19 (1995).
- [21] K. A. Trick and T. E. Saliba, *Carbon* **33**, 1509–1515 (1995).
- [22] K. A. Lincoln, *AIAA Journal* **21**, 1204–1207 (1983).
- [23] D. R. Allan, S. J. Clark, A. Dawson, P. A. McGregor, and S. Parsons, *Acta Cryst.* **B58**, 1018–1024 (2002).
- [24] V. E. Zavodnik, V. K. Bel’skii, and P. M. Zorkii, *Zh. Strukt. Khim.* **28**, p. 175 (1987).
- [25] A. Stukowski, *Modelling Simul. Mater. Sci. Eng.* **18**, p. 015012 (2010).

- [26] M. Frenkel, R. D. Chirico, V. Diky, X. Yan, Q. Dong, and C. D. Muzny, *J. Chem. Inf. Model.* **45**, 816–838 (2005).
- [27] V. Diky, C. D. Muzny, E. W. Lemmon, R. D. Chirico, and M. Frenkel, *J. Chem. Inf. Model.* **47**, 1713–1725 (2007).
- [28] K. G. Kroenlein, C. D. Muzny, V. Diky, R. D. Chirico, J. W. Magee, I. M. Abdulagatov, and M. D. Frenkel, Nist/trc web thermo tables (wtt) nist standard reference subscription database, 2011.
- [29] E. W. Lemmon, I. Bell, M. L. Huber, and M. O. McLinden, NIST Standard Reference Database 23: Reference Fluid Thermodynamic and Transport Properties-REFPROP, Version 10.0, National Institute of Standards and Technology, 2018.
- [30] H. L. Freidman, *J. Polym. Sci. C* **6**, 183–195 (1964).
- [31] K. A. Trick, T. E. Saliba, and S. S. Sandhu, *Carbon* **35**, 393–401 (1997).
- [32] H. Jiang, J. Wang, S. Wu, B. Wang, and Z. Wang, *Carbon* **48**, 352–358 (2010).
- [33] R. B. B. and, *J. Chem. Eng. Data* **10**, p. 143 (1965).
- [34] D. L. Cunha, J. A. P. Coutinho, J. L. Daridon, R. A. Reis, and M. L. L. Paredes, *J. Chem. Eng. Data* **58**, 2925–2931 (2013).
- [35] C. A. Buehler, J. H. Wood, D. C. Hull, and E. C. Erwin, *J. Am. Chem. Soc.* **54**, 2398–2405 (1932).